A partial review of semi-Lagrangian methods for the Vlasov equation

Nicolas Besse

Observatoire de la Côte d'Azur, Nice, France

Nicolas.Besse@oca.eu

Contents

The Vlasov equation (plasma setting)

- $(x, \xi) \in \mathbb{R}^d \times \mathbb{R}^d$, $d = 1, ..., 3$: the phase-space
- $f(t, x, \xi)$: the statistical distribution function of particles
- Vlasovian regime: $(\nu_{coll}/\omega_p) \sim g = (n_0 \lambda_D^3)^{-1} \ll 1$:
  Individual and short-range interactions (collisions) are neglected. Collective and long-range Coulombian interactions are dominant and modelized by mean-fields:

$$\frac{\partial f}{\partial t} + v(\xi) \cdot \nabla_x f + (F_{\mathrm{self}}(t, x, \xi) + F_{\mathrm{applied}}(t, x, \xi)) \cdot \nabla_\xi f = 0$$

The relativistic velocity $v(\xi)$ is given by:

$$v(\xi) = \frac{\xi / m}{\sqrt{1 + |\xi|^2/(mc)^2}}.$$

$F_{\mathrm{self}}(t, x, \xi)$ is the Lorentz force given by:

$$F_{\mathrm{self}}(t, x, \xi) = q(E(t, x) + v(\xi) \times B(t, x)).$$

The charge and current density are given by the two first moments of f

$$\rho(t,x) = q\int_{\mathbb{R}^d} f(t,x,\xi)d\xi, \qquad j(t,x) = q\int_{\mathbb{R}^d} v(\xi)f(t,x,\xi)d\xi.$$

The Vlasov-Poisson system (VP) (plasma case):

$$B = 0, \;\; E = -\nabla\phi, \;\; -\Delta\phi = \rho/\varepsilon_0$$

The Vlasov-Quasistatic system (VQS):

$$E = -\nabla\phi, \;\; -\Delta\phi = \rho/\varepsilon_0, \qquad B = \nabla\times A, \;\; -\Delta A = \mu_0 j.$$

The Vlasov-Darwin system (VD):

$$\begin{cases} \dfrac{\partial E_{irr}}{\partial t} - c^2\nabla\times B = -\mu_0 c^2 j, \quad \dfrac{\partial B}{\partial t} + \nabla\times E_{sol} = 0, \\ \nabla\cdot E_{irr} = \rho/\varepsilon_0, \quad \nabla\times E_{irr} = 0, \quad \nabla\cdot E_{sol} = 0, \quad \nabla B = 0, \\ E = E_{irr} + E_{sol} \end{cases}$$

The Vlasov-Maxwell system (VM):

$$\begin{cases} \dfrac{\partial E}{\partial t} - c^2\nabla \times B = -\mu_0 c^2 j, \quad \dfrac{\partial B}{\partial t} + \nabla \times E = 0, \\ \nabla \cdot E = \rho/\varepsilon_0, \quad \nabla \cdot B = 0. \end{cases}$$

For (VQS), (VD) and (VM) we have the compatibility condition for the source terms:

$$\frac{\partial \rho}{\partial t} + \nabla \cdot j = 0.$$

Other Vlasov systems:

- Vlasov-gravitational:
  Vlasov-Poisson, Vlasov-Nordström, Vlasov-Einstein, ...
- Vlasov-plasma, classic and quantum versions:
  Vlasov-waves, Vlasov-gyrokinetic,
  Vlasov-Wigner, Vlasov-Dirac-Benney, ...

Invariants

- $f_0(x,\xi) \geq 0 \Longrightarrow f(t,x,\xi) \geq 0, \ \forall t > 0$
- If f and β enough regular,

$$\int \beta(f(t,x,\xi)) \, dxd\xi$$

- Especially the norm L^p, $1 \leq p \leq \infty$

  $L^\infty \Longrightarrow$ maximum principle
  $L^1 \Longrightarrow$ mass conservation
  $L^2 \Longrightarrow$ numerical dissipation
- $\beta(r) = r \ln r \Longrightarrow$ "Boltzmann" kinetic entropy conservation

$$H(t) = \int f(t,x,\xi) \ln f(t,x,\xi) dxd\xi.$$

- Energy conservation:

$$(\mathrm{VP}): \qquad \frac{1}{2m} \int f(t,x,\xi)|\xi|^2 \, dxd\xi + \frac{\varepsilon_0}{2} \int |E(t,x)|^2 \, dx,$$

(VM):

$$\int mc^2(\gamma(\xi)-1)f(t,x,\xi)|\xi|^2\, dxd\xi \;+\varepsilon_0 \int \frac{|E(t,x)|^2+c^2|B(t,x)|^2}{2}\, dx$$

(VD):

$$\int mc^2(\gamma(\xi)-1)f(t,x,\xi)|\xi|^2\, dxd\xi \;+\varepsilon_0 \int \frac{|E_{irr}(t,x)|^2+c^2|B(t,x)|^2}{2}\, dx$$

- momentum conservation:

(VP):

$$\int f(t,x,\xi)\xi\, dxd\xi$$

(VM):

$$\int f(t,x,\xi)\xi\, dxd\xi + \int\; dx\; \varepsilon_0 E(t,x)\times B(t,x)$$

(VD):

$$\int f(t,x,\xi)\xi\, dxd\xi + \int\; dx\; \varepsilon_0 E_{irr}(t,x)\times B(t,x)$$

Characteristic curves equations

If $a(t,x,\xi) = (v(\xi), F(t,x,\xi))^T$ is enough regular (Lipschitz), we can introduce characteristic curves $(X(t;s,x,\xi), \Xi(t;s,x,\xi))$ associated to the first differential operator

$$\frac{\partial}{\partial t} + a.\nabla_{(x,\xi)}$$

which solves the classical ODEs equations

$$\begin{cases} \dfrac{dX}{dt}(t;s,x,\xi) = v(\Xi(t;s,x,\xi)), \\ \dfrac{d\Xi}{dt}(t;s,x,\xi) = F(t, X(t;s,x,\xi), \Xi(t;s,x,\xi)), \\ X(s;s,x,\xi) = x, \;\; \Xi(s;s,x,\xi) = \xi, \end{cases}$$

In the case of (VP), (VQS), (VD) and (VM), as

$$\nabla_{(x,\xi)} \cdot a = 0$$

the jacobian of the map

$$(x,\xi) \mapsto (X,\Xi) = \varphi_t(x,\xi) = (X(t;s,x,\xi),\Xi(t;s,x,\xi)),$$

remains constant and the Lagrangian flow $\varphi_t(x,\xi)$ preserves the measure and the connexity of the phase-space volume during time (phase-space incompressibility). This property implies the equivalence between the advective and the conservation form of the Vlasov Eq.:

$$\partial_t f + a \cdot \nabla_{(x,\xi)} f = 0 \quad \Longleftrightarrow \quad \partial_t f + \nabla_{(x,\xi)} \cdot (af) = 0,$$

which traduces conservation of the matter (continuity equation in phase-space). The advective form traduces the fact that f is constant along characteristic curves

$$f(t,x,\xi) = f(s,X(s;t,x,\xi),\Xi(s;t,x,\xi)).$$

RK: When variables are non-canonical φ_t is no more a volume-preserving map; the defect is compensated by the jacobian of the map "canonical $\leftrightarrow$non-canonical", but the flow is intrinsically volume-preserving (Liouville Th.)

A brief history of semi-Lagrangian methods for Vlasov (1/2)

- Introduced as first-order scheme by Courant-Issacson-Rees CPAM 52.
- Well developped in earlier time in the numerical-weather-prediction community: Wiin-Nielsen (Tellus 59), Robert (Atmosphere-Ocean 81), Staniforth, Coté, Smolarkiewicz, Priestley, Wood, Lauritzen, ...
- In plasma, for (VP) system, the first advective semi-Lagrangian method using cubic-splines and splitting is due to Cheng-Knorr JCP 76, and after Gagné-Shoucri JCP 77.
- In fluid mechanics and gas-dynamics, SL-methods (PPM methods) were developped by Colella-Woodward JCP 84.
- Sonnendrücker-Roche-Bertrand-Ghizzo JCP 98: advective-SL with cubic-splines and without splitting for Vlasov equation.
- Nakamura-Yabe CPC 99, CIP method: advective-SL with Hermite interpolation and transport of gradients of the distribution function.
- Conservative-SL method with Lagrange interpolation (1 to 3) FCT, FB & PFC methods: Boris-Book JCP 76, Laprise-Plante MWR 95, Mineau-Fijalkow CPC 99, Filbet-Sonnendrücker-Bertrand JCP 01.
- First advective-SL methods of high-order (Lagrange and Hermite type interpolation) on unstructured meshes: Besse-Sonnendrücker JCP 03.

A brief history of semi-Lagrangian methods for Vlasov (2/2)

- Comparisons of some different SL-methods and other methods: Mangeney et al JCP 02, Arber-Vann JCP 02, Filbet-Sonnendrücker CPC 03, Pohn-Shoucri-Kamelander CPC 05.
- Zerroukat-Wood-Staniforth IJMNF 06, PSM method: conservative-SL with cubic-splines.
- Conservative-SL with ENO-WENO reconstruction: Carillo-Vecil JSC 07, Qiu-Christlieb JCP 10, Qiu-Shu CiCP 11.
- Other conservative-SL methods using different filters to preserve positivity and limit oscillations: Yabe et al MWR 01, CPC 00, JCP 01; Crouseilles et al (PSM method) JCP 10; Umeda et al CPC 12.
- AMR SL-methods: Besse et al JCP 08, Mulet-Vecil JCP 13.
- Forward semi-Lagrangian method (similar to PIC methods): Denavit JCP 72, Leslie-Purser MWR 95, Nair-Scroggs-Semazzi JCP 03, Crouseilles et al JCP 09, ...
- Semi-Lagrangian discontinuous-Galerkin method: Restelli et al JCP 06, Mehrenberger et al ESAIM Proc. 11, Qiu-Shu JCP 11, Heath et al JCP 11, Rossmanith-Seal JCP 11, Tumolo et al JCP 13, Guo-Qiu JCP 13, Guo-Nair-Qiu MWR 14, Besse et al JCP 17, ...

Time discretization and operator splitting

- Consider the conservative Vlasov Eq. where $z = (z_1, z_2)$ are all the phase-space variables, and its splitting along the space z_1 and z_2, then

$$\partial_t f + \nabla_{z_i} \cdot (a_i(t,z) f) = 0, \quad i = 1, 2. \tag{1}$$

- If

$$\nabla_{z_i} \cdot a_i = 0, \quad i = 1, 2,$$

(which is not true in general) then conservative-splitting (1) is equivalent to the advective-splitting

$$\partial_t f + a_i(t,z) \cdot \nabla_{z_i} f = 0, \quad i = 1, 2, \tag{2}$$

otherwise it is equivalent to

$$\partial_t f + a_i(t,z) \cdot \nabla_{z_i} f = -f \, \nabla_{z_i} \cdot a_i(t,z), \quad i = 1, 2. \tag{3}$$

The right-hand sides of (3) compensate exactly since $\nabla \cdot a = 0$. But if it is not the case numerically (because the scheme is not well designed), it generates spurious error which can lead to numerical instabilities or physically wrong solutions in long-time!

$$f(t,z) = \mathcal{S}(t-s)f(s,z) = f\left(s, \varphi_t^{-1}(z)\right).$$

The splitting consists in approximating the evolution operator $\mathcal{S}(t)$. For $i = 1,2$, let $\mathcal{S}_i$ be the evolution operator associated to transport operator $A_i = a_i \cdot \nabla_{z_i}$.

1) The Lie-splitting, globally of order 1:

$$\begin{aligned} f(t+\Delta t) &= \mathcal{S}(\Delta t)f(t) = \mathcal{S}_2(\Delta t) \circ \mathcal{S}_1(\Delta t)f(t) + \mathcal{O}(\Delta t^2) \\ &= \exp(\Delta t A_2)\exp(\Delta t A_1)f(t) + \mathcal{O}(\Delta t^2). \end{aligned}$$

2) The Strang-splitting, globally of order 2:

$$\begin{aligned} f(t+\Delta t) &= \mathcal{S}(\Delta t)f(t) = \mathcal{S}_1(\Delta t/2) \circ \mathcal{S}_2(\Delta t) \circ \mathcal{S}_1(\Delta t/2)f(t) + \mathcal{O}(\Delta t^3) \\ &= \exp(\Delta t/2 A_1)\exp(\Delta t A_2)\exp(\Delta t/2 A_1)f(t) + \mathcal{O}(\Delta t^3). \end{aligned}$$

3) Splitting of global order N:

(Yoshida PLA 90; Forest PLA 91; Goldman-Kaper SINUM 96; Blanes et al SISC 06, BSMA 08; Schaeffer SINUM 09, Watanabe et al PoP 04, Christlieb et al CMS 11, Einkemmer et al SINUM 14, Casas et al NM 17)

$$\begin{aligned} \mathcal{S}(\Delta t) &= \mathcal{S}_1(\alpha_1 \Delta t) \circ \mathcal{S}_2(\beta_1 \Delta t) \circ \ldots \circ \\ & \quad \mathcal{S}_1(\alpha_k \Delta t) \circ \mathcal{S}_2(\beta_k \Delta t) + \mathcal{O}(\Delta t^{N+1}) \end{aligned}$$

The advective (backward) semi-Lagrangian method

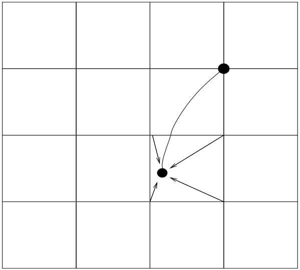

- f is conserved pointwise along characteristics.
- Find the origin of the characteristics ending at grids points:
  - Exact integration sometimes (using splitting)
  - ODEs solvers (Runge-Kutta, Adams-Bashforth, ...) $\Longrightarrow$ fixed-point problem (Picard or Newton iteration schemes) and convergence issues.
- Interpolate old values of f at origin of characteristics from known grid values: Need for high-order interpolation (locality/cost, order/accuray, diffusivity/stability issues).
- Typical interpolation schemes:
  - Cubic splines (Cheng-Knorr, ...) or high-order B-splines
  - Hermite with transport of derivatives (Nakamura-Yabe)
  - Finite-element-type interpolation such as Lagrange and Hermite (with gradient transport) type interpolation (Besse-Sonnendrücker)
  - Wavelets basis such as interpolets (Besse-et-al.)
  - Radial basis functions (Behrens-Iske-Käser)

Exact integration of characteristics using operator-splitting

- In many cases splitting allows to solve a constant-coefficient advection at each split-step.
- For example, in the case of separable Hamiltonian $H(x,\xi) = K(\xi) + V(x)$, the Vlasov equation written in canonical-coordinates, with the matrix $\mathbb{J} = [0, I_3; -I_3, 0]$

$$\partial_t f = -\nabla_{(x,\xi)} \cdot (f \mathbb{J} \nabla_{(x,\xi)} H) = \{H, f\}_{(x,\xi)} = \partial_x H \partial_\xi f - \partial_\xi H \partial_x f$$

can be solved by using the following conservative advective-splitting

$$\partial_t f + \nabla_\xi K \cdot \nabla_x f = 0, \quad \partial_t f + \nabla_x V \cdot \nabla_\xi f = 0,$$

and since K (resp. V) does not depend on x (resp. ξ), characteristics can be easily solved explicitly.
- Example, (VP): $K = m\xi^2/2$ and $V = q\phi(t,x)$

First-order integration of characteristics

- In the general case we need to integrate the ODEs

$$\frac{dZ}{dt}(t) = a(t, Z(t)). \tag{4}$$

- Backward solution:
  Z^n is unknown and a^n is known on the grid points Z^{n+1}.
- Using first-order quadrature formula (left or right rectangle) to integrate the ODEs (4) on one time-step, we get:

$$Z^{n+1} - Z^n = \Delta t a^n(Z^n) \quad \text{or} \quad Z^{n+1} - Z^n = \Delta t a^{n+1}(Z^{n+1})$$

- No explicit solution:
  - case 1: fixed-point problem need to be solved
  - case 2: predictor-corrector method on a is needed to find a^{n+1}

A one step predictor-corrector second-order method

- solve characteristics defined by $d_t Z = a(t, Z)$
- Mid-point quadrature rules on one time-step:

$$Z^{n+1} - Z^n = 2\Delta t \, a^{n+1/2}(Z^{n+1/2}), \quad Z^{n+1} + Z^n = 2Z^{n+1/2} + \mathcal{O}(\Delta t^2)$$

- Now the unknown $a^{n+1/2}$ is obtained by a predictor-correction procedure $\Longrightarrow \tilde{a}^{n+1/2}$.
- Solve a fixed point problem (e.g. using a Picard or Newton iteration scheme) to compute Z^n such that

$$Z^{n+1} - Z^n = \Delta t \, \tilde{a}^{n+1/2} \left(\frac{Z^{n+1} + Z^n}{2} \right)$$

- Remark: Both predictor-correction and fixed point iterations are required.

Second-order method for (VP)

- Let us use (VP) system to illustrate the method without splitting.
- At time t^n, f^n and E^n are known at the grid points (X^{n+1}, V^{n+1}), while f^{n+1} and E^{n+1} need to be computed.
- We have to solve backward in time from t^{n+1} to t^n the ODEs

$$d_t X(t) = V(t), \quad d_t V(t) = E(t, X(t))$$

  by predicting E^{n+1} which is unknown.
- Predict $\widetilde{E}^{n+1}$ using continuity (charge-conservation) + Poisson or Ampère equation.
- For all grid points $(x_i, v_i) = (X^{n+1}, V^{n+1})$ compute (Verlet):
- 1) $V^{n+1/2} = V^{n+1} - \frac{\Delta t}{2}\widetilde{E}^{n+1}(X^{n+1})$ 2) $X^n = X^{n+1} - \Delta t V^{n+1/2}$
- 3) $V^n = V^{n+1/2} - \frac{\Delta t}{2}\widetilde{E}^n(X^n)$ 4) interpolate f^n at (X^n, V^n).
- which gives first approximation of $f^{n+1}(x_i, v_i) = f^n(X^n, V^n)$ that can be used to correct $\widetilde{E}^{n+1}$.
- Iterate until $\widetilde{E}^{n+1}$ is stabilized. Few iterations are required.

Problems with non conservative methods

- When non conservative splitting is used, the solver is not exactly conservative.
- It does generally not matter when the solution is smooth and well resolved by the grid, because high-order schemes ensure asymptotically ($h \to 0$) small deviations of invariants.
- When fine structures develop in nonlinear regime and are at some point locally not well resolved by the phase-space grid, spurious effects could appear such as:
- large deviations of invariants (mass, maximun principle, energy)
- spurious oscillations, loss of particles
- numerical instabilities (enhanced by relativistic acceleration)

The conservative (backward) semi-Lagrangian method

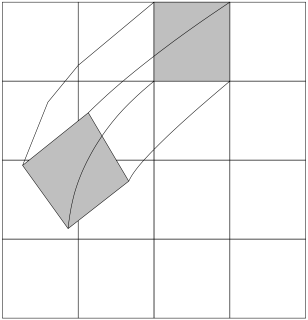

- We start with the Vlasov equation in conservative form

$$\partial_t f + \nabla \cdot (af) = 0.$$

- $\int_V f dx d\xi$ is conserved along characteristics.
- The algorithm decomposes in 3 steps:
  - transport backward the cells
  - High-order polynomial reconstruction from averaged values
  - Integration over transported cells
- Efficient with splitting in 1D conservative equation since a transported cell keeps the same topology: a segment defined by its 2 endpoints.
- Much more complex in nD ($n > 1$): topology of cells could change
- Splitting on conservative form leads to conservative algorithms
- No (or large) CFL number like advective-SL methods

Algorithm

- 1D-splitting with conservative-form equation
- Unknowns are cell averages:

$$f_i(t) = \frac{1}{h_i}\int_{z_{i-1/2}}^{z_{i+1/2}} f(t,z)dz, \quad h_i = z_{i+1/2} - z_{i-1/2}$$

- At time t^n, averages f_i^n are known
- Compute average values f_i^{n+1} on cells using

$$f_i^{n+1} = \frac{1}{h_i}\int_{z_{i-1/2}}^{z_{i+1/2}} f^{n+1}(z)dz = \frac{1}{h_i}\int_{Z(t^n;t^{n+1},z_{i-1/2})}^{Z(t^n;t^{n+1},z_{i+1/2})} f^n(z)dz$$

- Using the primitive $F_{h,m+1}^n(z) = \int_{z_{-1/2}}^{z} f_{h,m}^n(\zeta)d\zeta$, where $f_{h,m}^n(z)$ is a polynomial reconstruction of order m of f^n from averaged values f_i^n, the scheme then writes

$$f_i^{n+1} = F_{h,m+1}^n(Z(t^n;t^{n+1},z_{i+1/2})) - F_{h,m+1}^n(Z(t^n;t^{n+1},z_{i-1/2})),$$

with the properties $F_{h,m+1}^n(z_{i+1/2}) = \sum_{j=0}^{i} f_i^n$ and

$$F_{h,m+1}^n(z_{i+1/2}) - F_{h,m+1}^n(z_{i-1/2}) = h_i f_i^n = \int_{z_{i-1/2}}^{z_{i+1/2}} f_{h,m}^n(\zeta)d\zeta,$$

Backward transportation of the cells

- For 1D cell, we just need to compute the origins of characteristics which ends at the two end-points of the cell.
- Like in classical advective semi-lagrangian method discussed above.
- We must take care that end-points do not cross (change of topology), which implies a restriction on the time-step.

Reconstruction of the primitive $F_{h,m+1}(z)$ (1/2)

- Centered Lagrange interpolation of odd order $2d+1$

$$F_{h,2d+1}(z_\alpha) = \sum_{j=i-d}^{i+d+1} f_j L_j(\alpha), \quad i \le \alpha < i+1, \quad L_j(\alpha) = \prod_{k=j-d,\, k\neq j}^{j+d+1} \frac{\alpha - k}{j - k}$$

  - $d = 0$: Upwind scheme (under CFL$\leq$1)
  - $d = 1$: PFC scheme (Laprise-Plante MWR 95, Filbet-Sonnendrücker- Bertrand JCP 01)
  - For any d: shifted odd Strang scheme (Strang JMP 62, Strang-Iserles TAMS SINUM 83)

- ENO-WENO reconstruction (Lagrange interpolation with varying stencil): Carillo-Vecil JSC 07, Qiu-Christlieb JCP 10, Qiu-Shu CiCP 11.

- B-splines interpolation

$$F_{h,m+1}(z_\alpha) = \sum_{j\in Z} c_j(\{f_k\}) B_{m+1}(\alpha - j), \quad B_{m+1} = B_m * B_0, \quad B_0 = \mathbb{1}_{[-\frac{1}{2},\frac{1}{2}]}$$

For $m = 2$, PSM scheme (Zerroukat-Wood-Staniforth IJMNF 06)

Reconstruction of the primitive $F_{h,m+1}(z)$ (2/2)

- Hermite reconstruction: with $i \leq \alpha < i+1$

$$F_{h,3}(z_\alpha) = f_i + f_i'\alpha + (f_{i+1} - f_i - f_i')\alpha^2 + (f_{i+1}' + f_i' - 2(f_{i+1} - f_i))\alpha^2(\alpha - 1)$$

- Approximation of the derivative
  - $f_{i+}' = \frac{1}{6}(-f_{i+2} + 6f_{i+1} - 3f_i - 2f_{i-1})$
    $f_{i-}' = \frac{1}{6}(f_{i-2} - 6f_{i-1} + 3f_i + 2f_{i+1})$
    PFC scheme
    (Laprise-Plante MWR 95, Filbet-Sonnendrücker-Bertrand JCP 01)
  - $f_i' = \frac{1}{2}(f_{i-2} - f_{i+2} + 8(f_{i+1} - f_{i-1}))$
    PPM1 scheme (Colella-Woodward JCP 84)
  - $f_i' = \frac{1}{60}(f_{i+3} - f_{i-3} + 9(f_{i-2} - f_{i+2}) + 45(f_{i+1} - f_{i-1}))$
    PPM2 scheme (Colella-Sekora JCP 08)
  - $f_i : \quad \frac{1}{3}(f_{i+1}' + 4f_i' + f_{i-1}') = f_{i+1} - f_{i-1}$
    PSM scheme (Zerroukat-Wood-Staniforth IJMNF 06)

Positive reconstruction

- Physically, the distribution function is always positive.
- High-order interpolation can lead to negative values in some local areas.
- Reconstructed polynomial can be modified to remain positive.
- Theses modifications introduce a little more dissipativity, but far less as monotonic reconstructions performed in fluid dynamics.
- Some examples:
  - limitation of oscillations à la Colella-Woodward JCP 84
  - limitation of extrema using filters: Hyman SIMA JSSC 83, Umeda-Nariyuki-Kariya CPC 12
  - other limiters: Sureh-Huyng JCP 97, Zhang-Shu JCP 10, Hu-Adams-Shu JCP 13, Tanaka et al 17...

semi-Lagrangian discontinuous Galerkin methods

and

its AMR version

The principle of discontinuous-Galerkin method

0) We consider a 1D scalar conservation law, because the multi-dimensional case is solved by using splitting methods.

1) 1D scalar conservation law, $f = f(t,x)$,

$$\partial_t f + \partial_x (a(t,x) f) = 0 \quad + \text{initial conditions} + \text{boundary conditions}$$

2) We multiply the equation by a test fonction $\varphi \in V$, and we integrate on *each* cell I_i

$$\int_{I_i} (\partial_t f + \partial_x (af))\, \varphi \, dx = 0, \quad \forall \varphi \in V.$$

3) Weak formulation in space of the equation: integration by parts (IBP).

$$\int_{I_i} (\partial_t f \varphi - af \partial_x \varphi)\ dx + \int_{\partial I_i} af \cdot n \varphi \, d\gamma = 0, \quad \forall \varphi \in V.$$

4) Since V is a space of discontinuous functions, we replace fluxes by “numerical fluxes” at cell interfaces

$$\int_{I_i} (\partial_t f \varphi - af \partial_x \varphi)\ dx - (\widehat{af}\varphi)_{i-1/2} + (\widehat{af}\varphi)_{i+1/2} = 0, \quad \forall \varphi \in V$$

5) The choice of V (polynomial basis which can differ from a cell to another one) and numerical fluxes determine the properties of the numerical scheme (stability, convergence, high-order accuracy)

The semi-Lagrangian discontinuous Galerkin method (SLDG)

After time integration between t^n and t^{n+1} we get, with $f_h(t,x) = S_t(f_h^n)$ (where $S_t(f_h^n)$ is the exact evolution operator starting with the initial condition f_h^n),

$$\int_{I_i} f_h^{n+1} \cdot \varphi \, dx = \int_{I_i} f_h^n \cdot \varphi \, dx + \int_{t^n}^{t^{n+1}} \int_{I_i} a(t,x) S_t(f_h^n) \cdot \partial_x \varphi \, dx \, dt$$

$$- \int_{t^n}^{t^{n+1}} \left(a(t,x) S_t(f_h^n) \cdot \varphi|_{x^-_{i+1/2}} - a(t,x) S_t(f_h^n) \cdot \varphi|_{x^+_{i-1/2}} \right) dt.$$

A space-time integration by parts (Divergence theorem) of the conservation law on the domain $\Omega_{i-1/2}$ (cf. figure), transforms the time integration between t^n and t^{n+1} into a space integration (at time t^n) which uses origin of characteristic curves at time t^n (noted x^*).
This integral is evaluated by using a Gauss-Legendre quadrature formula:

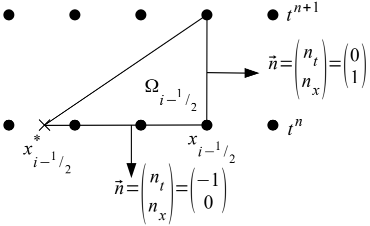

$$\int_{I_i} f_h^{n+1} \cdot \varphi \, dx = \int_{I_i} f_h^n \cdot \varphi \, dx + \Delta x_i \sum_{i_g} w_{i_g} \int_{\tilde{x}^*_{i_g}}^{\tilde{x}_{i_g}} f_h(\xi, t^n) \, d\xi \cdot \partial_x \varphi|_{\tilde{x}_{i_g}}$$

$$- \int_{x^*_{i+1/2}}^{x_{i+1/2}} f_h(\xi, t^n) \, d\xi \cdot \varphi(x^-_{i+1/2}) + \int_{x^*_{i-1/2}}^{x_{i-1/2}} f_h(\xi, t^n) \, d\xi \cdot \varphi(x^+_{i-1/2})$$

The characteristic discontinuous Galerkin method (CDG)

- Principle: we solve a dual problem. Indeed a test function $\varphi(x) \in V$ (taken as final condition at time t^{n+1}) is advected backward to the time t^n by the advection field $a(t, x)$. We then get:

$$\int_{I_i} f_h^{n+1}(x)\varphi(x)\,dx = \int_{I_i^*} f_h(t^n, x)\varphi(t^n, x)\,dx, \quad I_i^* = [x^*_{i-1/2}, x^*_{i+1/2}]$$

$$\approx \sum_{\ell} \sum_{i_g} w_{i_g} f_h(x^*_{i,\ell,i_g}, t^n)\varphi(x_{i,\ell,i_g})\Gamma(I^*_{i,\ell})$$

  - $x^*_{i\pm1/2}$: origin of characteristics at time t^n, coming from mesh points $x_{i\pm1/2}$ at t^{n+1}.
  - Index " ℓ " labels intersected cells.
  - Index " i_g " labels quadrature points (Gauss-Legendre).
  - $\Gamma(I^*_{i,\ell})$ is the measure of the intersection between cells I_i^* and I_ℓ.
- The method is illustrated by the following figure:

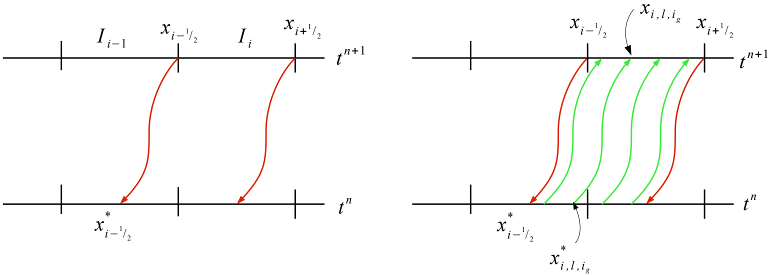

Principle of AMR

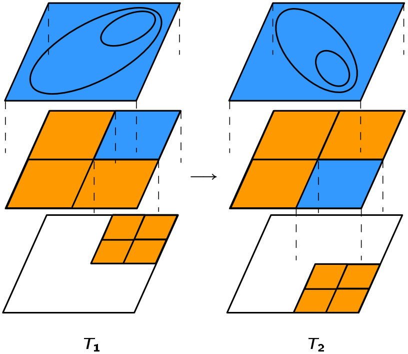

Example adaptive.

Black: level lines of the distribution function and mesh.

Blue: inactive cells, created but not used for computation.

Orange: active cells, created and used for computation.

Here, we see that 3 levels are created, two of which are used for computation.

The mesh is more refined where variations of level lines are important.

The typical loop of the algorithm:

- We suppose that we have an initial multi-wavelet representation of the distribution function associated to an initial (adaptive) mesh.
- Predict a new adaptive mesh by advecting forward (with a low-order scheme) cells of the initial mesh: Apply cell creation & cell refinement.
- Apply SLDG or CDG schemes by using the initial multi-wavelet representation of the distribution function projected on the predicted mesh. We then get a new multi-scale distribution function.
- Use a multi-wavelet decomposition of the new distribution function to discard details smaller than prescribed threshold: coarsening.

An example of adaptive mesh prediction

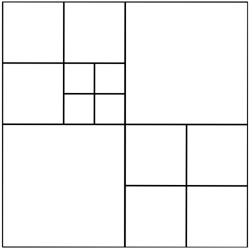

Initial mesh M^n.

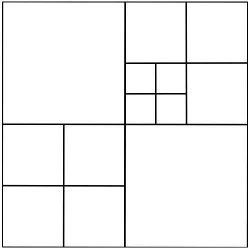

Predicted mesh after forward advection.

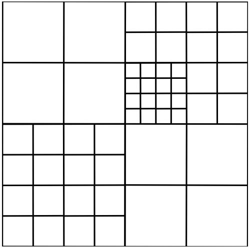

Predicted mesh after refinement.

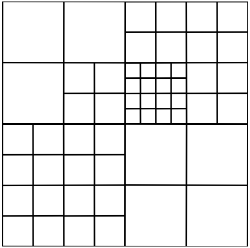

Merged mesh M^{n+1}.

Multi-scale representation by means of multi-wavelets basis

- We consider the spaces V_n^k of $\mathrm{Dim}(V_n^k) = 2^n k$ and defined by

$$V_n^k = \{f : \ f|_{[2^{-n}l, 2^{-n}(l+1)]} \in \mathbb{P}^k, \ l = 0, \ldots 2^n - 1, \ f \text{ elsewhere}\}, \ k \in \mathbb{N}, \ n \in \mathbb{N}.$$

- We have inclusions

$$V_0^k \subset V_1^k \subset \cdots \subset V_n^k \subset \cdots \subset L^2.$$

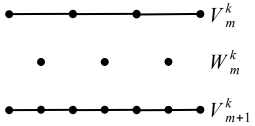

- The multi-wavelets space W_n^k is defined such that

$$V_{n+1}^k = V_n^k \oplus W_n^k \quad \text{and} \quad V_n^k \perp W_n^k.$$

- We then have the multi-scale decomposition:

$$V_n^k = V_0^k \oplus W_0^k \oplus W_1^k \oplus \ldots \oplus W_{n-1}^k,$$

or in other words the multi-scale representation of f:

$$f(t,x) = \sum_{j=0}^{k-1} \left(s_{j,0}^0(t)\phi_j(x) + \sum_{m=0}^{n-1} \sum_{l=0}^{2^m-1} d_{j,l}^m(t)\psi_{j,l}^m(x) \right)$$

- If $\{\phi_j\}_{j=0..k-1}$ is a basis for V_0^k then $\phi_{j,l}^n(x) = 2^{n/2}\phi_j(2^n x - l)$ is a basis for V_n^k.
  If $\{\psi_j\}_{j=0..k-1}$ is a basis for W_0^k then $\psi_{j,l}^n(x) = 2^{n/2}\psi_j(2^n x - l)$ is a basis for W_n^k.
- $s_{j,0}^0$: scale coefficient. $d_{j,l}^k$: wavelet coefficient.
- Threshold criterion: if $\|d_{\cdot,l}^m\|_{\ell^2} < \epsilon_m(\epsilon_0, m)$, then ignore details of level $\geq m$

Numerical results of the PhD of E. Madaule (JCP 332 2017)

Error for linear transport: rotation

threshold	$\langle h \rangle$	L^1 error	L^1 order	L^2 error	L^2 order	L^∞ error	L^∞ order
0.1	4.47	2.57	-	0.401	-	0.210	-
0.01	2.09	0.0523	5.10	0.0149	4.32	0.0173	3.27
0.001	1.14	5.98 E -3	4.43	1.39 E -3	4.14	1.52 E -3	3.60
1 E -4	0.529	6.31 E -4	3.89	1.46 E -4	3.71	2.94 E -4	3.08
1 E -5	0.236	6.53 E -5	3.60	1.42 E -5	3.48	2.84 E -5	3.03

Error obtained with the AMW-SLDG scheme for polynomials of degree 2.

threshold	$\langle h \rangle$	L^1 error	L^1 order	L^2 error	L^2 order	L^∞ error	L^∞ order
0.1	4.47	0.786	-	0.179	-	0.357	-
0.01	2.43	0.0118	6.87	3.72 E -3	6.33	6.81 E -3	6.47
0.001	2.09	5.85 E -3	6.42	1.34 E -3	6.42	1.72 E -3	6.99
1 E -4	1.23	1.38 E -3	4.92	3.03 E -4	4.95	4.63 E -4	5.16
1 E -5	0.625	7.11 E -5	4.73	1.76 E -5	4.69	4.22 E -5	4.59

Error obtained with the AMW-SLDG scheme for polynomials of degree 3.

threshold	$\langle h \rangle$	L^1 error	L^1 order	L^2 error	L^2 order	L^∞ error	L^∞ order
0.1	4.47	2.57	-	0.401	-	0.210	-
0.01	2.09	0.0538	5.07	0.0149	4.31	0.0184	3.19
0.001	1.14	7.87 E -3	4.23	1.77 E -3	3.97	1.67 E -3	3.54
1 E -4	0.527	6.90 E -4	3.85	1.45 E -4	3.71	2.81 E -4	3.09
1 E -5	0.236	1.31 E -4	3.36	2.36 E -5	3.31	2.84 E -5	3.03

Error obtained with the AMW-CDG scheme for polynomials of degree 2.

threshold	$\langle h \rangle$	L^1 error	L^1 order	L^2 error	L^2 order	L^∞ error	L^∞ order
0.1	4.47	0.787	-	0.179	-	0.357	-
0.01	2.43	0.0118	6.87	3.72 E -3	6.33	6.81 E -3	6.47
0.001	2.09	5.88 E -3	6.42	1.34 E -3	6.42	1.72 E -3	6.99
1 E -4	1.24	1.45 E -3	4.90	3.08 E -4	4.95	4.63 E -4	5.17
1 E -5	0.626	1.18 E -4	4.47	2.71 E -5	4.49	5.57 E -5	4.46

Error obtained with the AMW-CDG scheme for polynomials of degree 3.

Error for nonlinear transport: Burgers equation

threshold	$\langle h \rangle$	L^1 error	L^1 order	L^2 error	L^2 order	L^∞ error	L^∞ order
0.1	1.25	0.204	-	0.0860	-	0.0839	-
0.01	0.313	0.0105	2.14	3.80 E -3	2.25	3.54 E -3	2.28
0.001	0.157	1.30 E -3	2.43	4.78 E -4	2.50	4.65 E -4	2.50
1 E -4	0.0869	2.49 E -4	2.51	9.00 E -5	2.57	1.34 E -4	2.41
1 E -5	0.0412	2.40 E -5	2.65	8.28 E -6	2.71	1.00 E -5	2.64

Error obtained with the AMW-SLDG scheme for polynomials of degree 2.

threshold	$\langle h \rangle$	L^1 error	L^1 order	L^2 error	L^2 order	L^∞ error	L^∞ order
0.1	1.25	0.187	-	0.0612	-	0.0454	-
0.01	0.627	8.94 E -3	4.38	2.99 E -3	4.36	2.88 E -3	3.98
0.001	0.313	5.26 E -4	4.24	1.89 E -4	4.17	2.09 E -4	3.88
1 E -4	0.198	1.78 E -4	3.77	7.46 E -5	3.64	1.09 E -4	3.27
1 E -5	0.157	3.28 E -5	4.16	1.19 E -5	4.11	1.38 E -5	3.89

Error obtained with the AMW-SLDG scheme for polynomials of degree 3.

threshold	$\langle h \rangle$	L^1 error	L^1 order	L^2 error	L^2 order	L^∞ error	L^∞ order
0.1	1.25	0.204	-	0.0860	-	0.0839	-
0.01	0.313	0.0105	2.14	3.80 E -3	2.25	3.54 E -3	2.28
0.001	0.157	1.30 E -3	2.43	4.78 E -4	2.50	4.65 E -4	2.50
1 E -4	0.0869	2.48 E -4	2.52	9.00 E -5	2.57	1.34 E -4	2.41
1 E -5	0.0412	2.30 E -5	2.66	8.16 E -6	2.71	1.03 E -5	2.64

Error obtained with the AMW-CDG scheme for polynomials of degree 2.

threshold	$\langle h \rangle$	L^1 error	L^1 order	L^2 error	L^2 order	L^∞ error	L^∞ order
0.1	1.25	0.187	-	0.0612	-	0.0454	-
0.01	0.627	8.94 E -3	4.38	2.99 E -3	4.36	2.88 E -3	3.98
0.001	0.313	5.26 E -4	4.24	1.89 E -4	4.17	2.08 E -4	3.88
1 E -4	0.198	1.78 E -4	3.77	7.46 E -5	3.64	1.08 E -4	3.27
1 E -5	0.157	3.24 E -5	4.16	1.19 E -5	4.11	1.34 E -5	3.91

Error obtained with the AMW-CDG scheme for polynomials of degree 3.

Plasma case: bump-on-tail 1/2

I.C.: $f_0(x,v) = \dfrac{(1 + 0.04\cos(0.5x))}{10\sqrt{2\pi}} \left(9\exp\left(\dfrac{-v^2}{2}\right) + 2\exp\left(-2(v-4.5)^2\right)\right), \quad (x,v) \in [0, 20\pi] \times [-9, 9].$

$\Delta t = 0.1$. Maximum level of refinement is 8. Polynomial degree is 2. Threshold $\epsilon_0 = 3 \times 10^{-3}$.

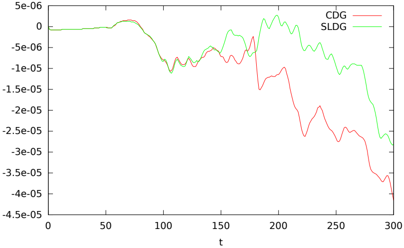

Relative variation of mass.

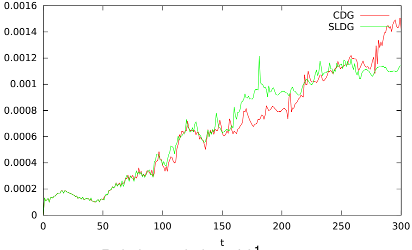

Relative variation of L^1-norm.

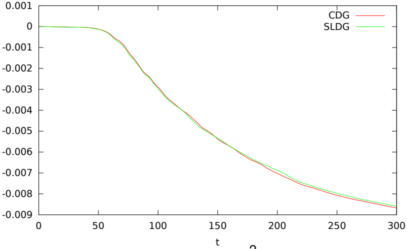

Relative variation of L^2-norm.

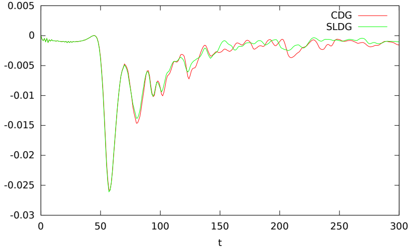

Relative variation of total energy.

Plasma case: bump-on-tail 2/2

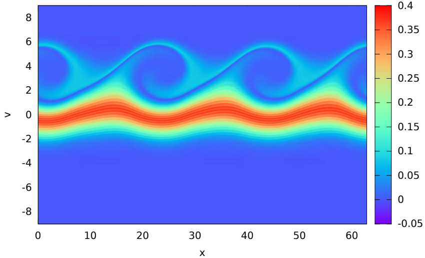

Distribution function at $t = 60$ pp.

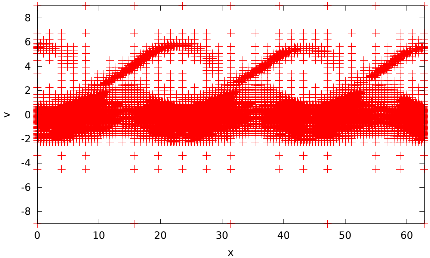

Mesh at $t = 60$ pp.

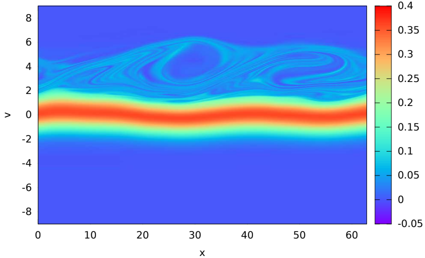

Distribution function at $t = 200$ pp.

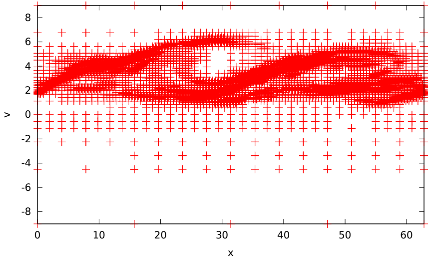

Mesh at $t = 200$ pp.

Distribution function and Mesh for bump on tail with the AMW-SLDG scheme.

Plasma case: focusing beam 1/2

Vlasov-Poisson equation with cylindrical symmetry:

$$\partial_t f(r,v,t) + \partial_r\left(\frac{v}{\varepsilon} f(r,v,t)\right) + \partial_v\Big(\left(E_\varepsilon(r,t) + F_\varepsilon(r,t)\right) f(r,v,t)\Big) = 0,$$

$$\frac{1}{r}\partial_r(rE_\varepsilon(r,t)) = \rho(r,t).$$

Initial Condition: $f_0(r,v) = \dfrac{3}{4v_{th}} \exp\left(\dfrac{-v^2}{2v_{th}^2}\right) \mathbb{1}_{[-1.8,1.8]}(r), \quad (r,v) \in [-3,3]^2.$

Focusing external field: $F_\varepsilon(r,t) = r\left(\dfrac{-1}{\varepsilon} + \cos^2\left(\dfrac{t}{\varepsilon}\right)\right).$

$\varepsilon = 0.1.$ $v_{th} = 0.07.$ $\Delta t = 0.02.$ Polynomials of degree up to 2.

Maximum level of refinement is 8. Threshold $\epsilon_0 = 10^{-2}$.

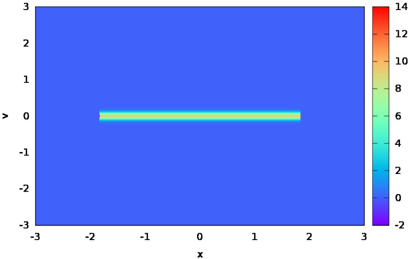

Initial distribution function.

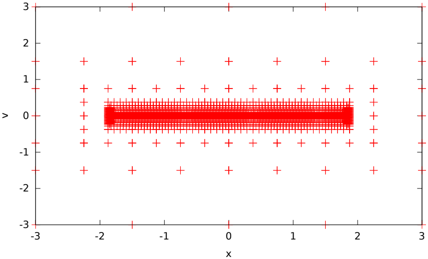

Initial mesh.

Plasma case: focusing beam 2/2

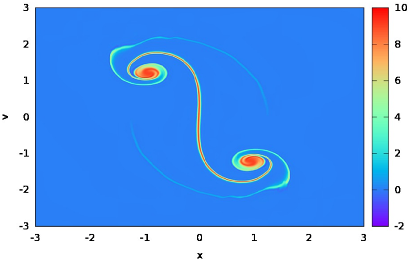

Distribution function at $t = 16$.

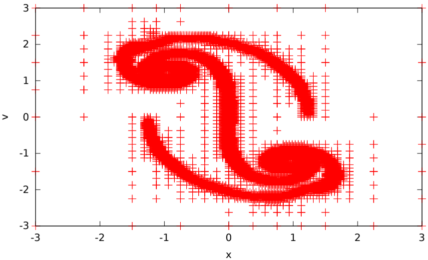

Mesh at $t = 16$.

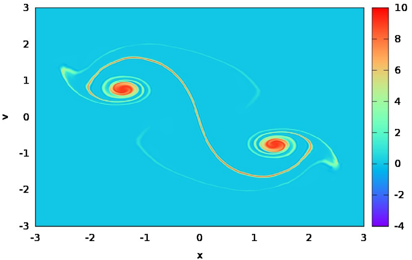

Distribution function at $t = 20$.

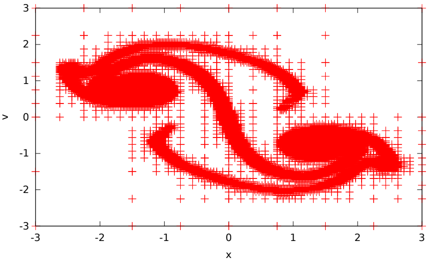

Mesh at $t = 20$.

Distribution function and mesh for focusing beam with the AMW-SLDG scheme.

Astrophysic case: cold layer 1/2

$$f_0(x,v) = \frac{1}{0.15\sqrt{2\pi}} \exp\left(-\frac{(v-u(x))^2}{2\times 0.15^2}\right), \quad (x,v)\in[0,2\pi]\times[-10,10],$$

$$u(x) = 0.01\sin(x).$$

$\Delta t = 0.02$.
Polynomials of degree 2.
Maximum level of refinement is 8.
Threshold is $\epsilon_0 = 3\times 10^{-3}$.

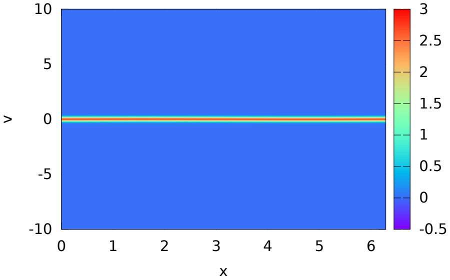

Initial distribution function.

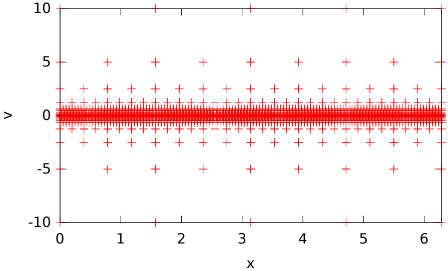

Initial mesh.

Astrophysic case: cold layer 2/2

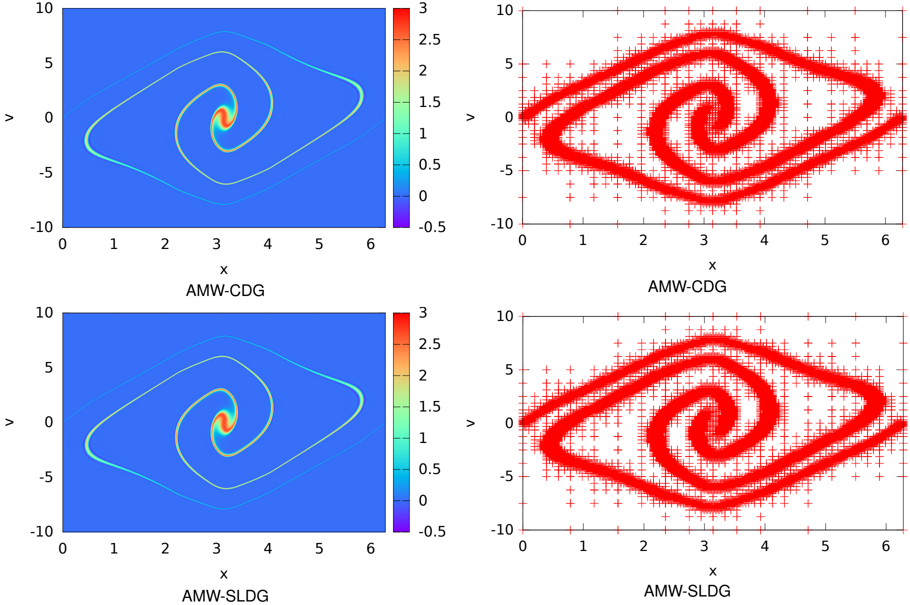

Distribution function and mesh at $t = 3$.

Astrophysic case: gaussian distribution 1/3

Initial condition: $f_0(x, v) = 4 \exp\left(-\frac{(x^2 + v^2)}{0.08}\right), \quad (x, v) \in [-2, 2]^2$

$\Delta t = 0.1$. Polynomials of degree up to 3. Maximum level of refinement is 9. Threshold is $\epsilon_0 = 3 \times 10^{-3}$.

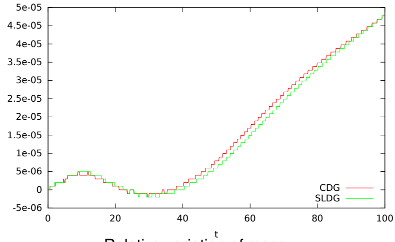

Relative variation of mass.

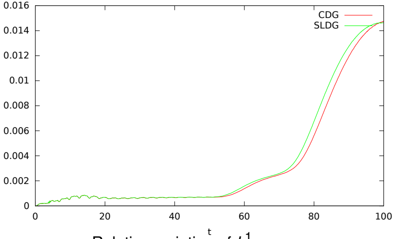

Relative variation of L^1-norm.

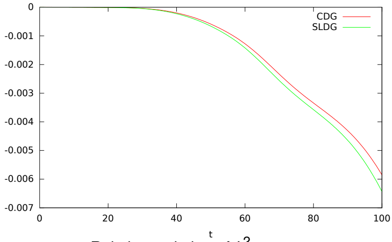

Relative variation of L^2-norm.

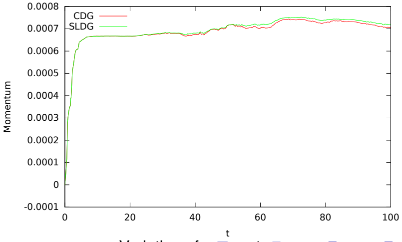

Variation of momentum.

Astrophysic case: gaussian distribution 2/3

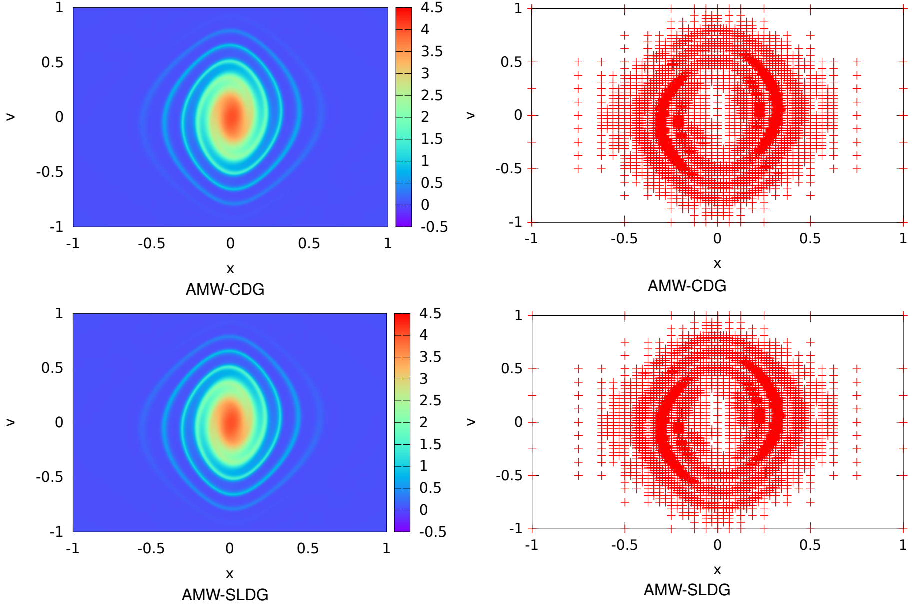

Distribution function and mesh at $t = 15$.

Astrophysic case: gaussian distribution 3/3

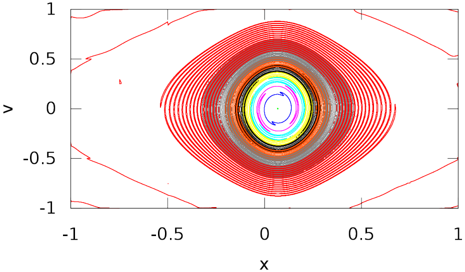

AMW-CDG

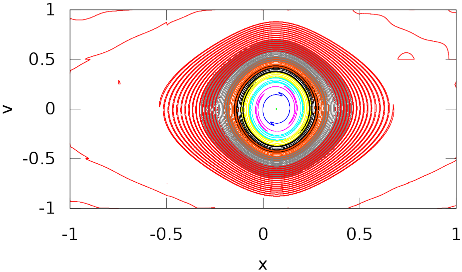

AMW-SLDG

Level lines of the distribution function at $t = 100$.

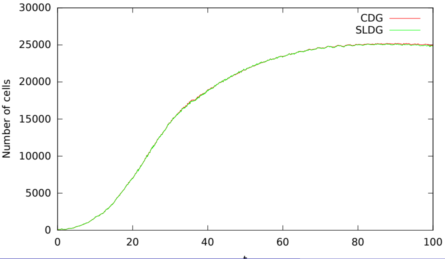

◀ Number of cells

- Adaptive mesh: 25000 cells
- Uniform mesh on $[-2, 2]^2$: 262000 cells
- Uniform mesh on $[-1, 1]^2$: 65500 cells

Astrophysic case: Jeans instability and return to BGK stationary state

$$f(x,v,0) = \frac{\exp\left(\frac{-v^2}{2}\right)}{\sqrt{2\pi}}(1 - A\cos(kx)), \quad (x,v) \in [0, 2\pi/k] \times [-V_c, V_c].$$

$A = 0.01, \quad k = 0.8 \quad$ and $\quad V_c = 6. \quad \Delta t = 0.1.$
Polynomials of degree 2.
Maximum level of refinement is 8.

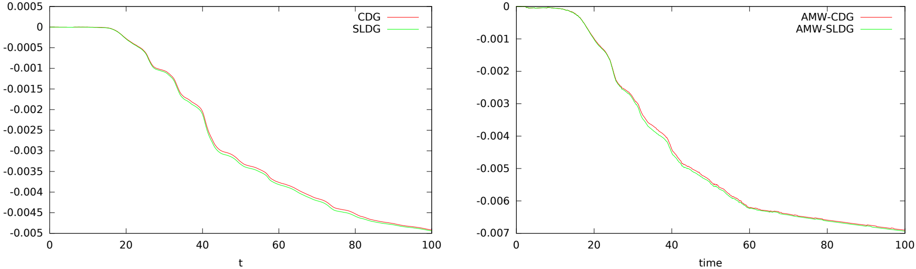

$\epsilon_0 = 0.003, \quad$ 8 refinement levels $\qquad \epsilon_0 = 0.01, \quad$ 7 refinement levels

Time evolution of L^2-norm

Astrophysic case: Jeans instability and return to BGK stationary state

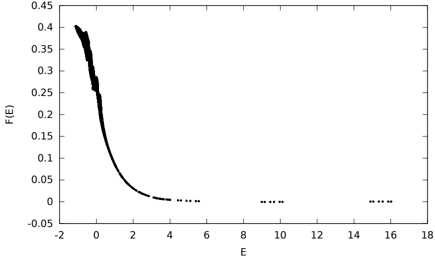

$E = v^2/2 - \phi(t = 100, x)$, $\epsilon_0 = 0.003$, 8 refinement levels

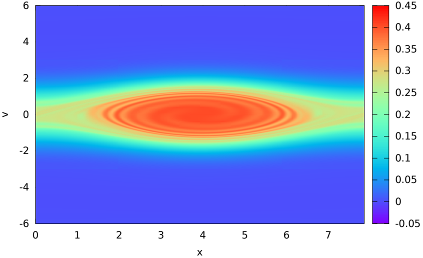

$f(t = 100, x, v)$, $\epsilon_0 = 0.003$, 8 refinement levels

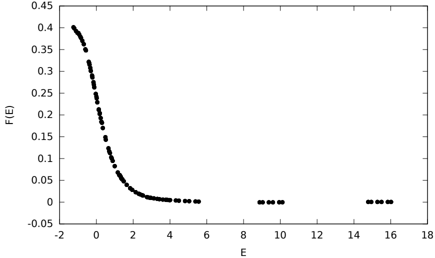

$E = v^2/2 - \phi(t = 100, x)$, $\epsilon_0 = 0.01$, 7 refinement levels

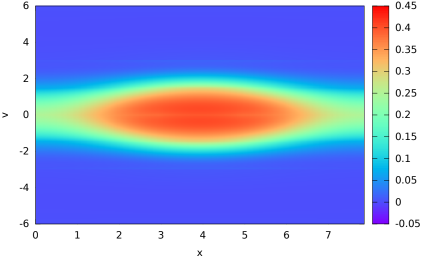

$f(t = 100, x, v)$, $\epsilon_0 = 0.01$, 7 refinement levels

AMW-CDG scheme

THANK YOU FOR YOUR ATTENTION